EVALUATION OF CRACK OCCURRENCE PROBABILITY OF T-SHAPE WELDED STRUCTURES

Y. Hsu [*]

General Education Center
Kainan University
Luchu, Taoyuan, Taiwan 33857, R.O.C.

W.-F. Wu [**] **H.-T. Kuo** [***]

Department of Mechanical Engineering
National Taiwan University
Taipei, Taiwan 10617, R.O.C.

ABSTRACT

Welded structures are vulnerable to fracture due to cracks, especially at the welds. To investigate the safety of T-Shape welded structures used in some construction sites, a method is proposed in this paper to evaluate the crack occurrence probabilities of the structures. Three major factors that affect the crack occurrence are taken into consideration. They are residual stress, diffusible hydrogen content and chemical composition of the weld metal. In the analysis, finite element analysis is performed to find the residual stress distribution of the structures. The uncertainties of diffusible hydrogen content and chemical composition are treated as random variables. The critical cooling time is found and utilized for evaluating the crack occurrence probability of the welded structure. Numerical results indicate that T-shape welded joints lead to higher residual stresses and higher crack occurrence probabilities in comparison with the traditional butt joints. Therefore, more attention should be paid to this kind of welded joints when they are used.

Keywords : Weld quality, Crack, T-shape welded joint, Crack occurrence probability.

1. INTRODUCTION

Welding is still an effective and economical way nowadays for joining metallic materials and has been widely applied in constructions. However, even though structure safety has been assured during design phase, possible crack initiation and growth resulted from the welding process can still impair the integrity of structures and might consequently lead to damage and danger to structures and human lives. Therefore, studies on the causes and related mechanical behaviors of the weld-cracks are quite necessary. One of the main causes for the occurrence of weld-cracks is the residual stress due to constraints exerted on the welded structures. It prohibits the free contraction of weld materials during the cooling process after heat is removed. Finite element method (FEM) has been used and proven its capability of calculating the residual stress distributions of welded structures by many researchers [1-4]. In particular, Wang *et al.* have simulated the deformation response of a thin-wall beam subjected to welding [5]. Analytical solutions [6] and empirical formulas [7] for estimating the residual stresses are also available, but their applications are restricted as compared to FEM when accuracy on stresses and suitability to various joint configurations are considered.

Another important factor causing weld-cracks is the residual diffusible hydrogen [8-12]. Part of the hydrogen elements contained originally in the weld electrodes may escape into the air during welding. Since the cooling process is so fast within the molten puddle, much of the hydrogen in atomic or ionic form will be entrapped and retained inside the weld materials. These hydrogen atoms or ions have smaller radii and, therefore, can move and diffuse freely within the metallic crystal lattices. They are apt to gather around tiny defects existing already within the materials. As the hydrogen concentration reaches a critical value, cracks start to appear and hydrogen gather furthermore at the crack tip leading to crack propagation and extension which eventually worsen joint strength between the weld metals. The larger the amount of hydrogen in weld electrodes, the higher the diffusible hydrogen

[*] Assistant Professor [**] Professor, corresponding author [***] Graduate student

DOI : 10.1017/jmech.2011.31
Copyright © 2011 The Society of Theoretical and Applied Mechanics, R.O.C.
https://doi.org/10.1017/jmech.2011.31 Published online by Cambridge University Press

content in weld metals, and the more probable cracks would occur. Therefore, electrodes with low hydrogen content are often required as part of the manufacturing specifications to reduce the possibility of crack occurrence. ISO 3690 classifies the hydrogen content within 5 ~ 10ml/100g as low when mercury-based measurement procedure suggested by International Institute of Welding (IIW) is adopted.

In addition, because of the elevated heat resulted from welding, the chemical composition and microstructures in the weld metals, having strong influences on weld-cracks, will change significantly, especially inside the region of heat affected zone (HAZ). Kuo *et al*. [13] have simulated the chemical and physical behaviors of heat affected zone in steel plates with low heat inputs. In the region of HAZ, the transformation process from smaller grains of austenite to larger ones of martensite leads to oversaturated solid-solutions of carbon-iron and makes the material more brittle and harder. Moreover, larger pores in martensite provide a better environment for diffusible hydrogen to aggregate. Both of the above factors increase the chances of crack occurrence. Thus, chemical constituents, especially carbon, as well as the brittleness and hardness characteristics in weld materials should be taken into account.

Yurioka *et al*. [14] proposed a set of equations in consideration of all three factors namely residual stress, diffusible hydrogen content and chemical composition as an evaluation base on the weld-crack occurrence. Deterministic single-valued data of all three of them are needed while using those equations. However, in reality, uncertainties concerning diffusion hydrogen content and chemical compositions exist and would affect the assessment of weld-crack occurrence and weld quality. Therefore, consideration of those uncertainties must be included. This study aims at predicting the probabilities of weld-crack occurrence of T-shape joints. T-shape joints are frequently used in welded constructions because of their structural stability as compared to simple butt joints. FEM is adopted to calculate weld residual stresses of different T-shape joint designs. Furthermore, uncertainties about chemical composition are considered and treated from probability and statistical viewpoints. Thus, a probability-based evaluation of the weld-crack occurrence is achieved.

2. CRACK OCCURRENCE CRITERION

2.1 Cooling Time, t_{100}

As mentioned in the preceding section, hydrogen is influential to weld-cracks. Some researchers have concluded that when the welding temperature ranges from −100°C to 100°C, hydrogen has its most adverse effect on welding [14-16]. They also pointed out that during the period when the welding temperature cools down from its peak to 100°C, the amount of diffusible hydrogen retained in the weld is crucial to the weld-crack occurrence. In the welding process, the cooling time for temperature to change from its peak to 100°C is denoted by t_{100} in the present study. The longer this cooling time takes, the more hydrogen can escape out of the weld, and the less likely cracks will occur. Nevasmaa [16] has discussed the influence of t_{100} on diffusible hydrogen content and cracking as well as their correlation. He suggested that t_{100} be used as a reference index for evaluating whether cracks will occur. In the present study, t_{100} will also be used as a reference index for predicting the possibility of weld-crack occurrence. If it exceeds a critical cooling time, cracks will not occur. On the other hand, if it is shorter than the critical cooling time, cracks will occur.

2.2 Critical Cooling Time, t_{cr}

Yurioka *et al*. [14] proposed a set of empirical equations for determining the above-mentioned critical cooling time denoted hereafter by t_{cr}. These equations, established through a large number of experimental data and statistical method, take all residual stresses, chemical compositions, and diffusible hydrogen into consideration. The expressions are as follows.

$$t_{cr} = \exp(67.6CI^3 - 182.0CI^2 + 163.8CI - 41.0) \tag{1}$$

in which

$$CI = CEN + 0.15\log H_{JIS} + 0.3\log(0.017K_t\,\sigma_w) \tag{2}$$

$$CEN = C + A(C)\cdot\left(\frac{Si}{24} + \frac{Mn}{6} + \frac{Cu}{15} + \frac{Ni}{20} + \frac{Cr + Mo + Nb + V}{5} + 5B\right) \tag{3}$$

$$A(C) = 0.75 + 0.25\tanh(20C - 2.4) \tag{4}$$

In the above Eq. (2), H_{JIS} indicates the measured diffusible hydrogen content when JISC Z 3113 standard is followed; $K_t\,\sigma_w$ is the residual stress estimated based on a simplified model proposed by Satoh and Ueda [7]. In Eqs. (3) and (4), *C*, *Si*, *Mn*, *Cu*, *Ni*, *Cr*, *Mo*, *Nb*, *V* and *B* are weight percentages of chemical contents of the weld metal; CEN, representing the degree of hardness and brittleness of the weld material, is a calculating function constructed from a modified carbon equivalent measurement method [14]. To have more accurate residual stress estimation, FEM will be used instead of Satoh and Ueda's simplified model in the present study.

The equations proposed by Yurioka *et al*. for t_{cr} will be applied to our case study since ranges of the chemical composition and the diffusible hydrogen contents of our case coincide with those of theirs. In the present study, comparison of t_{100} and t_{cr} will be made and used as the criterion for predicting whether weld-cracks will arise. When t_{100} is shorter than t_{cr}, crack occurrence is expected; while when t_{100} is longer than t_{cr}, no cracks will form.

3. RESIDUAL STRESS CALCULATION

3.1 Problem Description

Residual stresses inside welded structures are be-

https://doi.org/10.1017/jmech.2011.31 Published online by Cambridge University Press

lieved to be a major cause of cracking. To predict crack occurrence, the residual stress level should be pursued as accurately as possible. Therefore, instead of using approximate residual stress estimation formulas proposed by previous researchers, FEM is performed in the present study. The case study herein comes from a large-scaled metal structure as partly shown in Fig. 1. The unit's ring-like grid sheets stacked together and connected by welding make up the whole cylindrical construction. For such a construction, T-shape joints such as the one depicted in Fig. 2 are seen everywhere. For a typical T-shape joint, it is composed of three panels namely a, b and c, also shown in Fig. 2. Since cracking in the T-shape welded joints would significantly threaten the safety of the whole structure, the residual stresses inside the T-shape joints and in the neighborhoods of the welds need to be analyzed in detail.

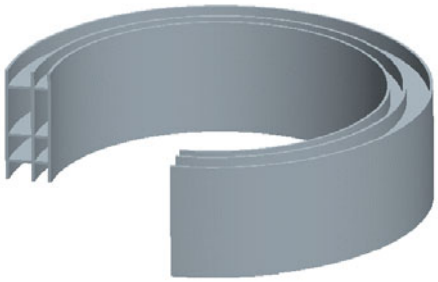


Fig. 1 Cylindrical metal structure

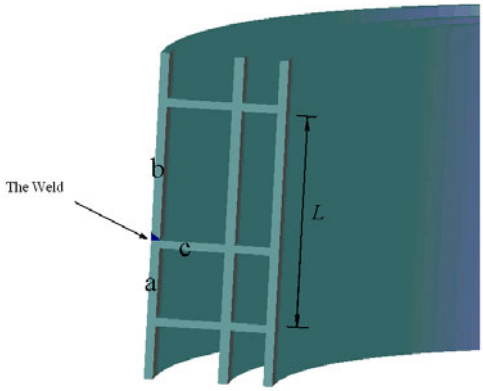


Fig. 2 Schematic diagram of weld and T-shape joint

3.2 Finite Element Models

As can be seen in Fig. 1, although the structure has a cylindrical shape, the ratio of cylindrical-radius to plate-thickness is quite high, and the radius is large compared with the length of the reinforcing plate c, it is reasonable to regard the curved plates *a* and *b* as flat plates. Furthermore, in reality, once a crack initiates, it would propagate and extend quite far along the weld in the circumferential direction, thus, an analysis solely on a T-shape welded cross-section located in the middle of the weld is representative enough. A real three dimensional (3D) T-shape structure is then mechanically simplified to a two dimensional (2D) plain strain model as shown in Fig. 3 to save simulation time.

Figure 4 is the geometrical dimensions of a real T-shape joint to be analyzed. To further understand how the location of plate *c* would affect the residual stress values and its distribution as well as the weld quality of the T-shape joint, another three cases with different locations of plate c (see Figs. 5 to 7) will also be analyzed, in which the total length of plate *a* and plate *b*, the length of plate c and the weld bevel remain unchanged. These four cases are labeled as P-1_a, P-1_m, P-1_r and P-1_l, respectively. Furthermore, a case of butt joint without plate *c* is added to the analysis. This case as that shown in Fig. 8 and labeled P-2 can help showing the difference of residual stress distribution and weld quality with and without plate *c*. Since researches on T-shape joint cases were few while many were on butt joint cases, to compare simulated results of our butt joint case with those of previously published butt joint cases can verify our numerical performance and further enhance the reliability of our FEM and numerical algorithm when T-shape joint cases are carried out.

A transient thermal-stress coupled-field finite element analysis with four-node plain strain elements was carried out. Figure 9 shows finite element meshes of T-shape joints. To consider the accuracy and efficiency of simulation, finer meshes were generated around the weld. Each end of the plates in T-shape joints was fixed. Low alloy and high strength steel,

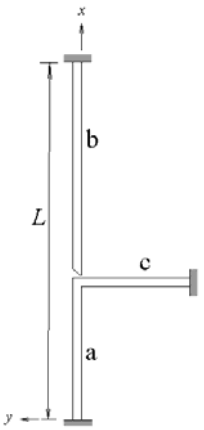


Fig. 3 2D T-shape structure case

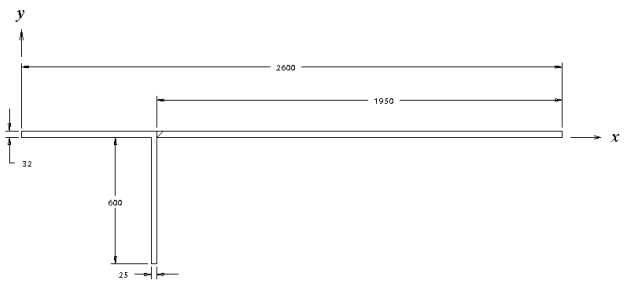


Fig. 4 P-1_a case

https://doi.org/10.1017/jmech.2011.31 Published online by Cambridge University Press

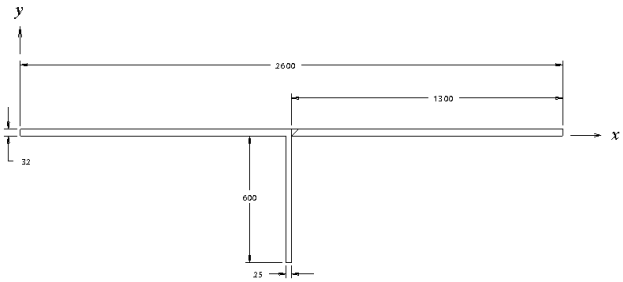


Fig. 5 P-1$_m$ cas

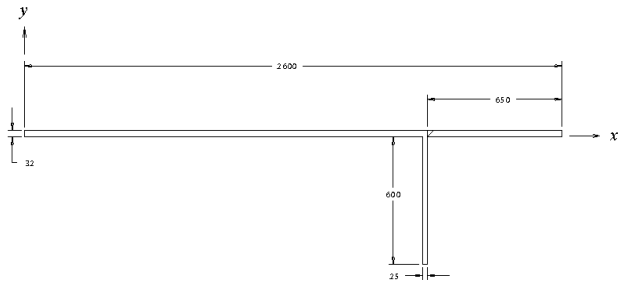


Fig. 6 P-1$_r$ case

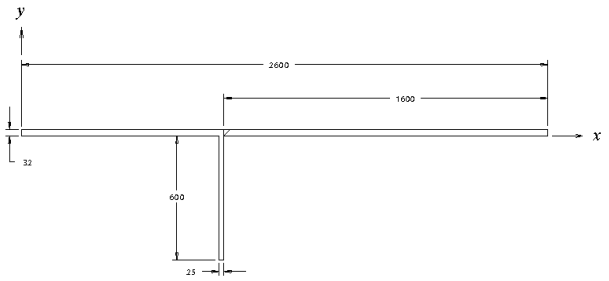


Fig. 7 P-1$_l$ case

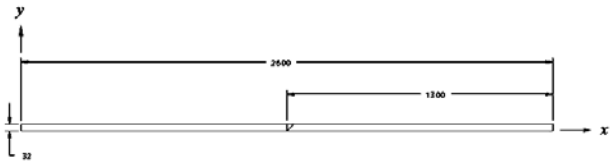


Fig. 8 P-2 case

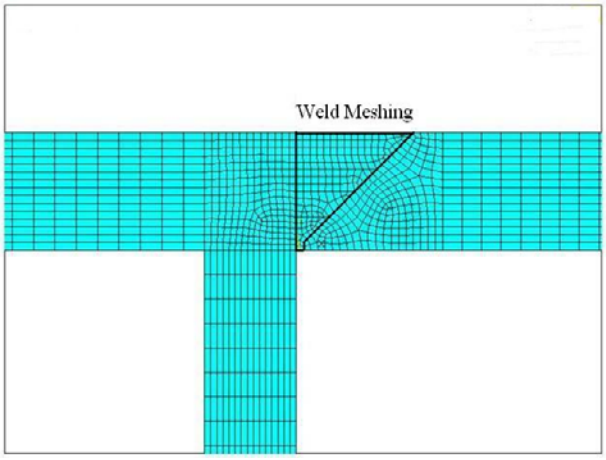


Fig. 9 Meshes around the weld

A533 Type B Class 2 specified by ASTM [17] was adopted whose mechanical properties and chemical compositions are listed in Table 1 and thermal physical properties such as thermal expansion, specific heat, *etc*. are shown in Fig. 10.

3.3 Loading Conditions

In real site construction, the surfaces of weld metals are preheated to 150°C before welding. Shielded Metal Arc Welding (SMAW) is then carried out using low hydrogen electrodes with heat input of 30kJ/cm. After welding, the heat source is removed and the welded structure cools down naturally without post heat treatment.

In the finite element modeling, the starting time of preheating procedure initiates a transient analysis of FEM. First, preheating of 150°C was imposed on the outer surface near the weld for 1,800 seconds. Afterwards, a 30-kJ/cm thermal energy with heat transfer efficiency of 0.75 was introduced into the weld for another 15 seconds [18]. The heat source was then removed, but the analysis did not stop until the welding temperature cooled down to the room temperature, 25°C.

3.4 FE Analysis Results

Figure 11 shows a typical local stress profile σ_x of P-2 case along *x*-direction near the weld. The weld bevel is located at the position about 0.058m in the figure where very high tensile stress appears. The stress drops fast from this highest value along each side of the weld bevel to compressive stress with the increase of distance away from the weld bevel. It changes more gradually afterwards. This stress profile for butt joint case is consistent with that documented in Kou [18], which consequently support the accuracy of the FE analysis. It should be noted that because of the slightly geometrical asymmetry of our single-beveled weld, the stress profile in Fig. 11 is slightly asymmetric.

FEM simulations show that the residual stress distribution patterns of the four P-1 series are very similar to one another. It indicates that position of plate *c* in the T-shape joint affects the residual stress in the weld very little. The stress distribution of P-1$_a$ case at the time when the welding temperature cooled down to the room temperature is selected for demonstration and shown in Fig. 12(a). It can be seen that the maximum stress value occurs near the root of the weld bevel where the crack initiates in practice. It can also be seen that high stress levels also occur near the toe of the weld bevel. This phenomenon of high stress concentration in these two areas is in agreement with that mentioned in Satoh and Ueda [7]. With regard to P-2 case, the stress distribution pattern shown in Fig. 12(b) is very similar to those of P-l series but the stress level is different. As summarized and shown in Table 2, the maximum stress values for P-1 series ranging from 740 to 759MPa are much higher than that of 420MPa for P-2 case. It reveals that the introduction of plate *c* induces higher residual stresses in the weld and leads

https://doi.org/10.1017/jmech.2011.31 Published online by Cambridge University Press

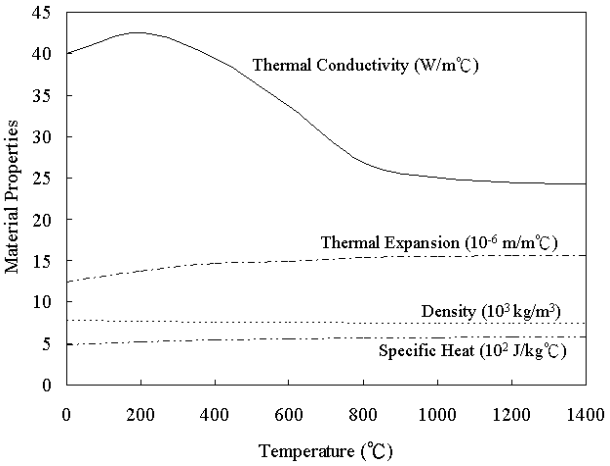


Fig. 10 Thermal physical properties of A533 Type B Class 2 [17]

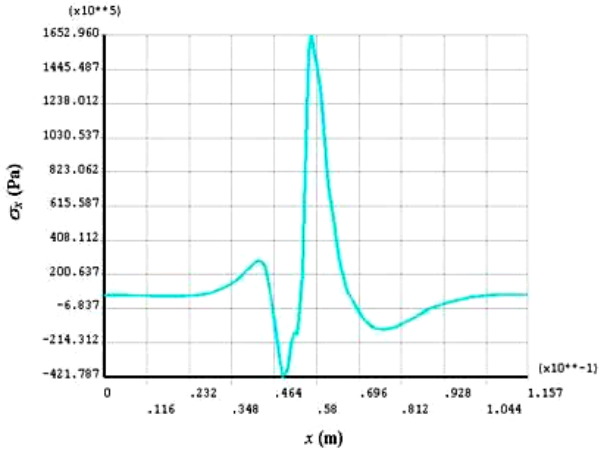


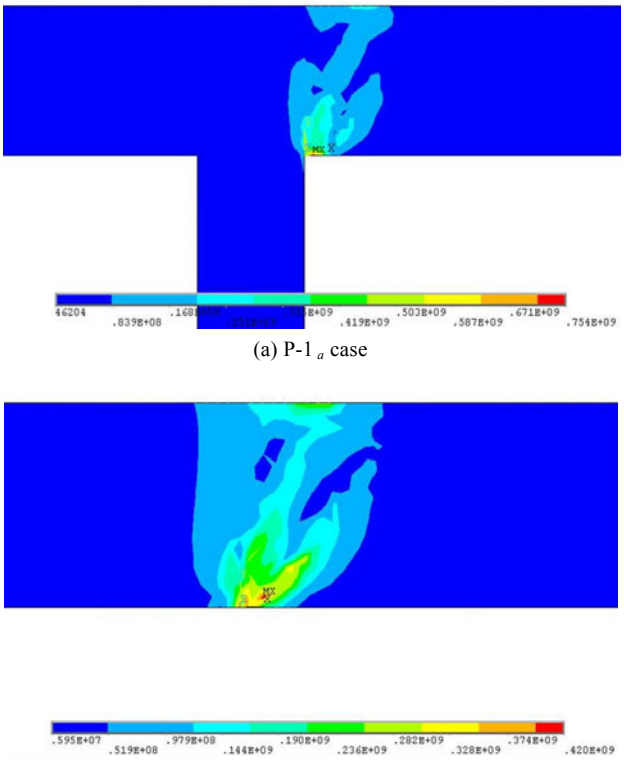
Fig. 11 Stress profile σ_x for P-2 case

more easily to weld-cracks. Although the plate *c* in the T-shape joint can truly enhance the rigidity and stability of the whole structure as compared with butt joint case, however, it also restricts free expansion or contraction of the welded structures during the welding and cooling processes, which consequently produces high residual stresses.

4. UNCERTAINTIES OF DIFFUSIBLE HYDROGEN AND CHEMICAL COMPOSITIONS

4.1 Uncertainty and Probability Distribution

In addition to residual stress, values of diffusible hydrogen content H_{JIS} as well as percentages of various chemical compositions are required to be incorporated into Eqs. (1) to (4) to calculate the critical cooling time t_{cr}. In this study, low hydrogen electrode is used for welding and thus the diffusible hydrogen content ranges from 5 to 10ml/100g according to IIW and ISO 3690. It should be noted that the diffusible hydrogen content in Eq. (2) is measured based on JIS Standards whose measurement method is different from that employed by International Institute of Welding (IIW). Suzuki and Yurioka proposed the following conversion relationship between these two standards [19].



(a) P-1 $_a$ case

(b) P-2 case

Fig. 12 Residual stress distribution

Table 1 Mechanical properties and chemical compositions of A533 Type B Class 2 required by ASTM [17]

Mechanical requirements	MPa
Tensile strength	795
Yield strength	485
Young's modulus	205×10^3
Chemical requirements	Composition, wt %
Carbon	0.25
Silicon	0.13-0.45
Manganese	1.07-1.62
Nickel	0.37-0.73
Molybdenum	0.41-0.64

Table 2 Simulated residual stresses

Structure cases	Max. σ_{res} (MPa)
P-1$_a$	754
P-1$_r$	759
P-1$_l$	747
P-1$_m$	740
P-2	420

https://doi.org/10.1017/jmech.2011.31 Published online by Cambridge University Press

$$H_{IIW} = 1.3H_{JIS} + 0.61 \quad (5)$$

with the help of Eq. (5), the diffusible hydrogen content H_{JIS} to be used in Eq. (2) is found in the range of 3.38 to 7.22ml/100g.

In general, the diffusible hydrogen content is not of deterministic value but having variability. Similarly, some chemical compositions listed in Table1 also vary to certain extents. In practice, even though the manufacture quality of metals and electrodes are well controlled, uncertainties still exist and can not be eliminated leading to the inevitable variability of chemical compositions and hydrogen content, and eventually having influence on the assessment of weld-crack occurrence. To deal with these uncertainties, probabilistic and statistical concepts are employed in this study.

No prior studies have specified the probability distributions of those diffusible hydrogen content and chemical compositions mentioned above. In the present study, normal probability distributions are assumed to describe the scattered values of the diffusible hydrogen and chemical compositions. The mean value μ and standard deviation σ are two parameters needed in specifying a normal distribution. The lower and upper limits of the diffusible hydrogen content or any specific chemical composition shown in Table 1 are herein assigned to be ±3σ plus its mean value since three-sigma is usually taken as the quality control limits in product monitoring processes in the industry. Consequently, μ can be determined by the average of lower and upper limits and σ can be obtained by the difference of lower and upper limits divided by six. For example, the mean value of the diffusible hydrogen content is 5.30ml/100g and the standard deviation is 0.64ml/100g when the diffusible hydrogen content ranges from 3.38 to 7.22ml/100g. In the study, H_{JIS} and four chemical compositions *Si*, *Mn*, *Ni* and *Mo*, making a total of five random variables are considered as uncertainty factors while other compositions are assumed to be zero in calculating the critical cooling time t_{cr}.

4.2 Monte Carlo Simulation of t_{cr}

Uncertainties of the diffusible hydrogen content and chemical compositions result in random t_{cr} instead of a deterministic value, indicating the existence of a specific probability distribution of t_{cr}. To obtain the distribution, sufficient t_{cr} data should be collected first. Monte Carlo simulation technique was employed in the present study. Each of the five random variables H_{JIS}, *Si*, *Mn*, *Ni* and *Mo* following the normal distribution with its own mean value and standard deviation stated previously were generated by MATLAB software and then incorporated into Eqs. (1) to (4) with other deterministic values including the numerically simulated residual stress, t_{cr} sample data were obtained. The number of sample data is suggested not to be less than 30 in some studies. Here, in order to obtain a smooth and accurate probability distribution of t_{cr}, the simulation process was run 1,000 times repetitively.

4.3 Chi-Square Test for Goodness-of-Fit

As stated above, 1,000 sample data of t_{cr} were obtained from Monte Carlo simulation. Three widely-used probability distributions namely normal, log-normal and Weibull distributions were chosen to fit the sample data. The parameters of these three distributions can be estimated by least-squared regression or curve fitting techniques stated in many books [20,21]. The detailed procedure is not described herein but can be referred to in Hu [22]. Table 3 tabulates the estimated parameters of each probability distribution for P-1 series and P-2 case.

To determine the best fittest probability distribution, the simulation data must be grouped first into several intervals. In each interval, there is a value of observed number of occurrence O_t coming from sample data and a corresponding value of expected number of occurrence E_i deduced from the hypothesized distribution. Chi-square test for goodness-of-fit was then conducted. The test statistic χ^2 is expressed as

$$\chi^2 = \sum_{i=1}^{k} \frac{(O_i - E_i)^2}{E_i} \quad (6)$$

where k is the number of distribution intervals, O_i represents the observed number of sample in the i-th interval, and E_i denotes the expected number of sample in the i-th interval. When the test statistic χ^2 satisfies the following condition, the data is believed to be fitted with the hypothesized distribution with a significance level of α.

$$\chi^2 < C_{1-\alpha,f} \quad (7)$$

in which f indicates the degree-of-freedom of the chi-square distribution, and C denotes the critical value of χ^2 corresponding to α and f. In this study, as three hypothesized distributions were used in fitting the probability distribution of t_{cr}, if there are more than one hypothesized distributions passing the test of goodness-of-fit, comparison of the test statistic χ^2 should be made further and the most appropriate probability distribution of t_{cr} can be decided with the smallest value of χ^2.

Table 4 summarizes results of the chi-square test for goodness-of-fit of t_{cr} where a significance level of 0.5% was selected. For each individual case, the one with symbol "◯" indicates the best-fitted probability distribution of t_{cr}. From Table 4, it is concluded that data of t_{cr} follows normal distribution for all P-1 series whereas lognormal distribution fits P-2 case the best.

5. PROBABILITY OF CRACK OCCURRENCE

In addition to residual stresses, the other important simulation result from FE analysis is the time duration t_{100} used in judging whether weld-cracks will occur or not. It is found that t_{100} ranges from 1,221 to 1,228 seconds in P-1 series and is 1,566 seconds for P-2 case. The reason why t_{100}'s for P-1 series are about 300

https://doi.org/10.1017/jmech.2011.31 Published online by Cambridge University Press

Table 3 Estimated parameters in probability distribution functions

Structure cases	Normal		Lognormal		Weibull	
	μ	σ	μ_{log}	σ_{log}	θ	β
P-1_a	1,501	262.7	7.299	0.181	1,605	7.002
P-1_r	1,515	339.4	7.271	0.241	1,604	5.273
P-1_l	1,513	259.9	7.307	0.178	1,616	7.106
P-1_m	1,456	257.1	7.268	0.182	1,558	6.913
P-2	9,25.3	217.6	6.802	0.244	1,005	5.165

Table 4 Chi-square test results for each simulation case

Structure cases	f	$C_{0.995,f}$	χ^2		
			Normal	Lognormal	Weibull
P-1_a	9	23.6	6.7	31.1	69.3
			○		
P-1_r	13	29.8	19.6	50.7	76.7
			○		
P-1_l	9	23.6	20.9	38.4	67.6
			○		
P-1_m	9	23.6	9.7	31.6	60.3
			○		
P-2	7	20.3	22.6	20.3	64.5
				○	

seconds less than that for P-2 case is due to the increase of total surface area with the additional reinforcing plate *c* and its location by the weld side. In P-1 series, the welding heat can be transmitted easily to the reinforcing plate making the dissipation of thermal energy faster and the welding structure more brittle as compared to that of P-2 case. When checking the cooling time documented in Yurioka *et al*. [14] for the butt joint, at the preheating temperature of 150°C and plate thickness of 32 mm, t_{100} is found to be around 1,500 seconds. It is quite consistent with that of our P-2 case calculated from FE numerical analysis. It once again verifies the accuracy of our FE modeling and analysis.

As stated in Section 2, crack occurrence probability is evaluated by comparing the process cooling time t_{100} with the critical cooling time t_{cr}. If t_{100} is less than t_{cr} indicating the process cooling time is not long enough, cracks will occur. Since the probability distribution of t_{cr} has been obtained, the probability of weld-crack occurrence can be determined by calculating the area in the interval $[t_{100}, \infty]$ of the probability density function of t_{cr}. Table 5 lists all t_{100} values and crack occurrence probabilities for the studied P-1 series and P-2 case. It can be seen that crack occurrence probabilities of P-1 series are all greater than 0.8, however, P-2 case only has the probability of 0.0053 for crack occurrence. It

Table 5 Cooling times and welding crack probabilities for simulated cases

Structure cases	t_{100} (sec)	Pr. ($t_{100} < t_{cr}$)
P-1_a	1,228	0.8518
P-1_r	1,230	0.8823
P-1_l	1,221	0.8705
P-1_m	1,225	0.8188
P-2	1,566	0.0053

indicates that although T-shape joints make the structure more stable but they result in higher risks of crack occurrence as compared to butt joints. In comparison among various P-1 cases, it is also found that the location of reinforcing plate c has no significant influence on the crack occurrence probability. If such a plate will be installed for the sake of structural stability, P-1_m is preferred among all P-1 series.

6. CONCLUDING REMARKS

This study investigates the effect of the welded joint configuration on the crack occurrence probability of the weld with the help of a critical cooling-time equation. Four P-1 serial cases with different positions of reinforcing web-plate in a T-shape joint and a butt joint P-2 case without the web-pale are considered. For each case, finite element method is employed to find the residual stress distribution in and around the weld as well as its maximum value. Uncertainties and variability of the diffusible hydrogen content and chemical compositions are taken into consideration and treated as random variables. The crack occurrence probabilities of different cases are obtained and compared with one another. Some conclusions are drawn as follows.

1. The structure models with the reinforcing plate (P-1 series, T-shape joints) have higher residual stresses than that of the case without reinforcing plate (P-2, butt joint). The stress levels of T-shape joints can reach up to about 750MPa which is very close to the tensile strength of material, whereas the stress level is only about 420MPa for butt joint case.
2. The time durations for welding process to cool down from its highest temperature to 100°C for P-1 series are about 300 seconds less than that for P-2 case. It is owing to the faster energy dissipation during cooling down process with the inclusion of the reinforcing plate.
3. By chi-square test of goodness-of-fit, it is found that probability distributions of critical cooling time for P-1 series follow the normal distribution while that for P-2 case is the lognormal one.
4. The crack occurrence probabilities for P-1 series are all greater than 0.8 while only 0.0053 for P-2 case. It reveals that T-shape joints are much vulnerable to cracks than the butt joints although they can

https://doi.org/10.1017/jmech.2011.31 Published online by Cambridge University Press

strengthen the rigidity and stabilize the whole structure from mechanical point of view.

5. The reinforcing plate c does have significant effect on the residual stresses and crack occurrence probabilities of the welded structures. Its location, however, does not seem to be relevant.

ACKNOWLEDGMENTS

Most of the computation work in this paper was carried out by Mr. C.L. Hu. The authors are grateful to him for the help.

REFERENCES

1. Free, J. A. and Goff, F. D. P., "Predicting Residual Stresses in Multi-Pass Weldments with the Finite Element Method," *Computers & Structures*, **32**, pp. 365–378 (1989).
2. Li, Y. J., Wang, J., Chen, M. and Shen, X., "Finite Element Analysis of Residual Stress in the Welded Zone of a High Strength Steel," *Bulletin of Materials Science*, **27,** pp. 127–132 (2004).
3. Teng, T. L. and Chang, P. H., "Three Dimensional Thermo-Mechanical Analysis of Circumferentially Welded Thin-Walled Pipes," *International Journal of Pressure Vessels and Piping*, **75**, pp. 237–247 (1998).
4. Lindgren, L. E., "Finite Element Modelling and Simulation of Weldingm, Part 1, Increased Complexity," *Journal of Thermal Stresses*, **24**, pp. 141–192 (2001).
5. Wang, Y. X., Zhang, P., Hou, Z. G. and Li, C. Z., "Inherent Strain Method and Thermal Elastic-Plastic Analysis of Welding Deformation of a Thin-Wall Beam," *Journal of Mechanics*, **24**, pp. 301–309 (2008).
6. Khraishi, T. and Jing, P. H., "Analytical Solutions for Crack Tip Plastic Zone Shape Using the von Mises and Tresca Yield Criteria: Effect of Crack Mode and Stress Condition," *Journal of Mechanics*, **20**, pp. 199–210 (2004).
7. Satoh, K. and Ueda, S., "Studies on Structural Restraint Severity Relating to Weld Cracking in Japan," IIW Doc. X-808-76, 197626, International Institute of Welding (1976).
8. Okuda, N., Nishikawa. Y., Aoki. T., Goto, A. and Abe, T., "Hydrogen-Induced Cracking Susceptibility of Weld Metal," IIW Doc. II-1072-86/II-A-86, International Institute of Welding (1986).
9. Nevasmma, P. and Karppi, R., "Implications on Controlling Factors Affecting Weld Metal Hydrogen Cold-Cracking in High-Strength Shielded-Metal Arc (SMAW) Multipass Welds Metal," IIW Doc. IX-1997-01, International Institute of Welding (1997).
10. Nevasmma, P., "Controlling Factors Affecting Hydrogen Cold Cracking in High-Strength Multi-Pass Weld Metals—Comparison of the Cracking Test Results between SMAW and SAW Welds," IIW Doc. IX-2027-02, International Institute of Welding (2002).
11. Yurioka, N., "Predictive Methods for Prevention and Control of Hydrogen Assisted Cold Cracking," IIW Doc. IX-1938-99, International Institute of Welding (1999).
12. Granjon, H., *Fundamentals of Welding Metallurgy,* Abington Publishing, U.K. (1991).
13. Kuo, H. T., Wei, R. C., Wu, W. F. and Yang, J. R., "Simulated Heat Affected Zone in ASTM A533-B Steel Plates under Low Heat Inputs," *Materials Chemistry and Physics*, **117**, pp. 471–477 (2009).
14. Yurioka, N., Suzuki, H., Ohshita, S. and Saito, S., "Determination of Necessary Preheating Temperature in Steel Welding," *Welding Journal*, **62**, pp. 147s–153s (1983).
15. Hart, P. H. M. and Watkinson, E., "Weld Metal Impact Test Ranks Cr-Mo Hydrogen Cracking Resistance," *Welding Journal*, **54,** pp. 288s–295s (1975).
16. Nevasmaa, P., "Predictive Model for the Prevention of Weld Metal Hydrogen Cracking in High-Strength Multipass Welds," Ph.D. Dissertation, Department of Mechanical Engineering, University of Oulu, Oulu, Finland (2003).
17. ASTM, "Standard Specification for Pressure Vessel Plates, Alloy Steel, Quenched and Tempered, Manganese-Molybdenum and Manganese-Molybdenum-Nickel (A533/A533M-93)," American Society for Testing and Materials (1999).
18. Kou, S., *Welding Metallurgy*, John Willey & Sons, U.S.A. (1987).
19. Suzuki, H. and Yurioka, N., "Prevention against Cold Cracking in Welding Steels," *Australian Welding Journal*, **27**, pp. 9–17 (1982).
20. Ebeling, C. E., *An Introduction to Reliability and Maintainability Engineering*, McGraw-Hill, U.S.A. (1997).
21. Ang, A. H. S. and Tang, H. W., *Probabilistic Concepts in Engineering Planning and Design*, John Wiley & Sons, U.S.A. (1984).
22. Hu, C. L., "Delayed Cracking Analysis in Welding Structures," Master Thesis, Department of Mechanical Engineering, National Taiwan University, Taipei, Taiwan (2005).

(Manuscript received December 21, 2009, accepted for publication January 28, 2010.)

https://doi.org/10.1017/jmech.2011.31 Published online by Cambridge University Press